

***N*-representability and variational stability in natural orbital functional theory**

John M. Herbert^{a)} and John E. Harriman^{b)}

Theoretical Chemistry Institute and Department of Chemistry, University of Wisconsin, Madison, Wisconsin 53706

(Received 19 February 2003; accepted 25 March 2003)

Several “reconstructive” proposals for density matrix functional theory are investigated, each of which expresses the two-electron density matrix, and therefore the electronic energy, as a functional of the natural orbitals and their occupation numbers. It is shown that for each of these functionals, half of the parallel-spin eigenvalues of the reconstructed two-electron density matrix are necessarily negative. Illustrative all-electron calculations for Be and LiH, in a variety of Gaussian basis sets, demonstrate that these spurious negative eigenvalues lower the electronic energy substantially. In spite of this, there is no indication that the variationally optimized energy diverges as the basis set approaches completeness, as has been suggested based on calculations with a small number of active orbitals. The apparent variational instability reported previously is attributed to qualitative differences between the minimal-basis and extended-basis potential curves, for certain functionals. However, we identify one functional that yields accurate LiH potential curves—comparable to full configuration interaction results—in both minimal and extended basis sets. Explicitly antisymmetric reconstructions are recommended as a remedy for the positivity problem. © 2003 American Institute of Physics. [DOI: 10.1063/1.1574787]

I. INTRODUCTION

Following a flurry of activity that produced many formal results¹ but no actual calculations, one-electron density matrix functional theory (DMFT) languished for many years, but now interest in this topic has been rekindled by a number of explicit proposals^{2–9} for calculating electronic energies as functionals of the natural orbitals and their occupation numbers, that is, as functionals of the one-electron reduced density matrix (1-matrix). DMFT does not rely upon any noninteracting reference state and therefore incorporates fractional occupation numbers in a natural way, which may provide the necessary infrastructure for an even-handed description of both dynamical and nondynamical correlation. Moreover, by eliminating the rigid distinction between occupied and virtual orbitals, DMFT provides a means to generate localized, weakly occupied pseudonatural orbitals^{10–12} to replace Hartree–Fock (HF) or Kohn–Sham virtual orbitals in compact expansions of correlated wave functions.

Several recent proposals for DMFT^{4–7,13–15} constitute, at least implicitly, a sort of generalized HF theory in which the two-electron reduced density matrix (2-matrix) \hat{D} is expressed as a functional $\hat{D}[\hat{\gamma}]$ of the 1-matrix $\hat{\gamma}$. Given such a *reconstruction functional*, the electronic energy is determined by variational minimization of the functional $E[\hat{\gamma}] = \text{tr}(\hat{H}\hat{D}[\hat{\gamma}])$. This brand of “reconstructive” DMFT amounts to a variational 2-matrix theory where—in an effort to reduce the exorbitant computational expense¹⁶ inherent to such calculations—the 2-matrix is parametrized in terms of the 1-matrix. Ensemble *N*-representability constraints¹⁷ for

acceptable 1-matrices are easy to implement, but are insufficient to guarantee that the reconstructed 2-matrix is *N*-representable. Hence the burden of 2-matrix *N*-representability falls on the reconstruction functional.

This perspective on DMFT has interesting parallels in density functional theory (DFT), where parametrizations of the exchange–correlation hole, as a functional of the electron density, figure prominently in the development of new energy functionals.^{18–23} Only for an exact reconstruction of the hole is one assured that $E \leq E[\rho_{\text{trial}}]$, whereas $E \leq E[\hat{\gamma}_{\text{trial}}]$ would be guaranteed in DMFT only if the exact reconstruction $\hat{D}[\hat{\gamma}]$ could be employed. For practical approximations there is no lower bound, at the theorem level, on either $E[\rho_{\text{trial}}]$ or $E[\hat{\gamma}_{\text{trial}}]$. DFT survives as a viable methodology because, empirically, the energy does converge with respect to enlargement of the variational space.^{24–26} Thus, while the variationally optimized energy in approximate DFT may be higher or lower than the exact energy, the model exchange–correlation hole is at least associated with a finite energy in the complete-basis limit. Whether the model 2-matrices corresponding to proposed functionals $\hat{D}[\hat{\gamma}]$ exhibit this property—dubbed *variational stability*—was questioned in a recent study,²⁷ where it was determined that optimized DMFT energies for diatomic molecules decrease precipitously as the number of active orbitals is increased.

The aforementioned result is intriguing but not conclusive, because no more than six active orbitals were used for any molecule other than H₂. For H₂, extrapolation to the limit of a complete basis of *s* and *p* functions yields a reasonable result,¹⁴ but there has been no systematic study of the basis-set dependence of reconstructive DMFT for molecules that contain heavy atoms. The effect of higher angular

^{a)}Present address: Department of Chemistry, The Ohio State University, Columbus, OH 43210.

^{b)}Electronic mail: harriman@chem.wisc.edu

momentum basis functions also has not been scrutinized in a serious way. In addition, because existing reconstruction functionals fail to preserve antisymmetry of the 2-matrix, there are serious questions about their behavior for same-spin electrons,²⁸ which cannot be answered by examining H_2 . In the present work we study Be and LiH, which incorporate heavy atoms and same-spin electrons but are small enough so that large basis sets impart a great deal of variational flexibility.

Two questions are addressed in this work. First, does the variationally optimized electronic energy ultimately converge with respect to enlargement of the variational space? Our results indicate that it does. In fact, the decrease in DMFT energy with respect to basis-set enlargement is roughly comparable to that of full configuration interaction (FCI), although polarization functions in DMFT prove to be more effective in lowering the energy than they are in FCI. What appeared to be an instability in the small active-space calculations is instead the manifestation of a pronounced, qualitative discrepancy between the potential curves obtained using a minimal basis set and those calculated with extended basis sets. All of the functionals examined here yield qualitatively correct LiH potential curves in a minimal basis set, but in several cases these potentials become unrealistically shallow when extended basis sets are employed.

Second, we examine in detail the N -representability violations manifested by the variationally optimized 2-matrices. We give a general proof that half of the eigenvalues of $\hat{D}^{\alpha\alpha}$ (the parallel-spin component of \hat{D}) are necessarily negative for each functional examined here. In certain applications, the magnitude of the most negative eigenvalue approaches 30% of the largest positive eigenvalue, and in all cases the negative eigenvalues contribute substantially to the electronic energy. This behavior is inherent to the ansatz, but we shall argue that explicitly antisymmetric reconstruction functionals are likely to assuage this positivity problem.

II. RECONSTRUCTION FUNCTIONALS

We consider \hat{S}_z eigenstates of a spin-compensated (non-spin-polarized) N -electron system, wherein the natural spin-orbitals are direct products $|\varphi_k\rangle \otimes |\sigma\rangle$ and the 1-matrix has spin blocks $\hat{\gamma}^\alpha = \hat{\gamma}^\beta$, with

$$\hat{\gamma}^\alpha = \sum_k n_k |\varphi_k\rangle \langle \varphi_k|. \quad (1)$$

(Throughout this work, Greek indices are used for spin while Latin indices denote spatial orbitals.) Spin blocks

$$\hat{D}^{\sigma\mu} = \sum_{ijkl} D_{ij,kl}^{\sigma\mu} |\varphi_i \varphi_j\rangle \langle \varphi_k \varphi_l| \quad (2)$$

of the 2-matrix will be reconstructed in the natural orbital direct product basis, $|\varphi_i \varphi_j\rangle = |\varphi_i\rangle \otimes |\varphi_j\rangle$. In this basis the matrix elements of $\hat{D}^{\alpha\alpha}$ are antisymmetric,

$$D_{ij,kl}^{\alpha\alpha} = -D_{ji,kl}^{\alpha\alpha} = -D_{ij,lk}^{\alpha\alpha} = D_{ji,lk}^{\alpha\alpha}. \quad (3)$$

The elements of $\hat{D}^{\alpha\beta}$ possess no special symmetry because this matrix is only one component of the $\alpha\beta$ part of \hat{D} . The

TABLE I. Specification of reconstruction functionals, according to Eq. (6).

Functional	Refs.	$f(n_i, n_j)$
HF		$n_i n_j$
CH(ζ)	2, 5–7	$(n_i n_j)^{\zeta/2}$
SIC-CH(ζ)	4, 13, 15	$(n_i n_j)^{\zeta/2} + (n_i^2 - n_j^2) \delta_{ij}$
CHF(ζ)	5, 6, 32	$n_i n_j + \zeta \sqrt{\Delta_{ii} \Delta_{jj}}$
MCHF	6	$(n_i n_j + \sqrt{\Lambda_{ii} \Lambda_{jj}})/2$

complete opposite-spin part of \hat{D} consists of spin blocks $\hat{D}^{\alpha\beta} \equiv \hat{D}^{\alpha\beta\alpha\beta}$, $\hat{D}^{\alpha\beta\beta\alpha}$, $\hat{D}^{\beta\alpha\alpha\beta}$, and $\hat{D}^{\beta\alpha\beta\alpha}$, only one of which is permutationally independent.^{29,30} Generally, then, the 2-matrix contains three independent spin blocks: $\hat{D}^{\alpha\beta} \equiv \hat{D}^{\alpha\beta\alpha\beta}$, $\hat{D}^{\alpha\alpha} \equiv \hat{D}^{\alpha\alpha\alpha\alpha}$, and $\hat{D}^{\beta\beta} \equiv \hat{D}^{\beta\beta\beta\beta}$. The latter two are identical for spin-compensated systems, so in this work we deal only with $\hat{D}^{\alpha\alpha}$ and $\hat{D}^{\alpha\beta}$.

The 1- and 2-matrices are normalized such that $0 \leq n_k \leq 1$, $\text{tr } \hat{\gamma}^\alpha = N/2$, $\text{tr } \hat{D}^{\alpha\alpha} = N(N-2)/8$, and $\text{tr } \hat{D}^{\alpha\beta} = N^2/8$. The 1-matrix derives from the 2-matrix according to the sum rule

$$\gamma_{i,j}^\alpha = 2(N-1)^{-1} \sum_k (D_{ik,jk}^{\alpha\alpha} + D_{ik,jk}^{\alpha\beta}). \quad (4)$$

Existing reconstruction functionals for DMFT express the matrix elements $D_{ij,kl}^{\sigma\mu}$ as functions of the natural occupation numbers, neglecting any explicit dependence of $D_{ij,kl}^{\sigma\mu}$ on the natural orbitals themselves. This is driven partly by convenience, but also because HF theory leads to one such reconstruction, and because the energy functional already inherits a strong dependence on the natural orbitals, via the one- and two-electron integrals. This assumption may limit the present methods to spin-compensated states, because for a spin-polarized state the α -spin natural orbitals differ from the β -spin ones. In any case, a spin-restricted formalism is adopted here.

The reconstructions examined here each utilize the simple Hartree product

$$D_{ij,kl}^{\alpha\beta} = \frac{n_i n_j}{2} \delta_{ik} \delta_{jl} \quad (5)$$

for the opposite-spin component of the 2-matrix. For the parallel-spin component, the functionals of interest have the form

$$D_{ij,kl}^{\alpha\alpha} = \frac{1}{2} [n_i n_j \delta_{ik} \delta_{jl} - f(n_i, n_j) \delta_{il} \delta_{jk}]. \quad (6)$$

This implies an energy functional

$$E[\{n_k\}, \{|\varphi_k\rangle\}] = 2 \sum_i n_i h_{ii} + \sum_{ij} (2 n_i n_j \langle ij | ij \rangle - f(n_i, n_j) \langle ij | ji \rangle), \quad (7)$$

where h_{ij} and $\langle ij | kl \rangle$ denote one- and two-electron integrals in the $|\varphi_k\rangle$ basis.

Listed in Table I are the functions f that define the corrected Hartree (CH),^{2,5–7} corrected Hartree–Fock (CHF),^{5,6} and modified CHF (MCHF)⁶ functionals. The quantities

$$\Delta_{ij} = n_i(1 - n_j), \quad \Lambda_{ij} = n_i(2 - n_j) \quad (8)$$

have been introduced for succinctness. As advertised, the CH functional adds an exchange correction to $(\hat{\gamma} \otimes \hat{\gamma})/2$, the Hartree 2-matrix, albeit one that does not fully annihilate self-interaction in the Hartree potential. The CHF functional adds a correction to the HF 2-matrix²⁸ $\hat{\gamma} \wedge \hat{\gamma}$, in order to account for the two-electron cumulant.³¹ This cumulant vanishes for an idempotent 1-matrix.

The functionals introduced in Table I appear in the literature under a litany of pseudonyms, and the names introduced here are an attempt to unify this nomenclature. The functional CH(ζ) generalizes CH(1), which was derived independently by several authors,^{2,5,7} based on different criteria. The functional CHF(ζ) includes the scaling parameter ζ suggested by Staroverov and Scuseria³² (with an opposite sign convention), and recovers the original CHF functional⁵ when $\zeta=1$. SIC-CH(ζ) is a partially self-interaction-corrected version of CH(ζ), introduced^{13,14,33} as a generalization of the functional SIC-CH(1) proposed by Goedecker and Umrigar.^{4,15} [In previous work,²⁸ we referred to SIC-CH(ζ) as CP(ζ), and CH(ζ) was called SICP(ζ).]

SIC-CH(ζ) is obtained from CH(ζ) by deleting all “orbital” self-interactions⁴ (that is, all $D_{ii,ii}^{\alpha\alpha}$ matrix elements). SIC-CH(ζ) retains some residual *electron* self-interaction, however, insofar as this functional is not antisymmetric. The only antisymmetric reconstruction consistent with Eq. (6) is the HF one, $f(n_i, n_j) = n_i n_j$, which is equivalent to both CH(2) and SIC-CH(2).

A few values of the adjustable parameter ζ are chosen for the calculations in Sec. V. For CH(ζ) and SIC-CH(ζ), we choose $\zeta=1$ and $\zeta=4/3$. The latter value is an upper bound on the range of acceptable ζ for these functionals, as determined based upon electron-gas considerations,^{14,33} and produces more realistic electron-pair densities than those obtained using smaller values of ζ .²⁸ For CHF(ζ), we consider $\zeta=0.7$, $\zeta=1$, and $\zeta=1.12$. When $\zeta \approx 0.7$, CHF(ζ) yields diatomic potential curves with correct shape, while CHF(1.12) produces accurate energies for the Be isoelectronic sequence.³²

III. *N*-REPRESENTABILITY

Since the HF functional is the only antisymmetric reconstruction consistent with the ansatz in Eq. (6), none of the other functionals affords an *N*-representable 2-matrix. To gain a more incisive understanding of the *N*-representability violations, we analyze the so-called *D*, *Q*, and *G* conditions^{34–36} for the reconstructed 2-matrices. These constraints specify that the two-electron density matrix (\hat{D}), the two-hole density matrix (\hat{Q}), and the particle-hole density matrix (\hat{G}) must be positive (semidefinite). Because \hat{Q} and \hat{G} can be expressed in terms of \hat{D} , each constitutes a necessary requirement for an *N*-representable 2-matrix. Physically, the *Q*- and *G*-conditions place bounds on the occupancies of two-electron states that do not follow from the Pauli-Coleman bounds on the orbital occupancies.³⁴ Although these conditions are insufficient to guarantee that \hat{D} is *N*-representable, when taken together they are nevertheless quite strong, as indicated by the high quality of variational

2-matrix calculations constrained only by \hat{D} , \hat{Q} , and \hat{G} positivity.^{16,37–39} Sans *G*, the *D* and *Q* conditions are considerably less restrictive.³⁷

To specify these conditions, define an operator $\hat{P}^{\sigma\mu}$ with elements

$$P_{ij,kl}^{\sigma\mu} = \frac{1}{2} \langle \Psi | \hat{A}_{i\sigma, j\mu} \hat{A}_{k\sigma, l\mu}^\dagger | \Psi \rangle, \quad (9)$$

in which $\hat{A}_{i\sigma, j\mu}$ is a product of two creation and/or annihilation operators for the natural spin-orbital basis. $\hat{P}^{\sigma\mu}$ is the metric matrix for the states $\hat{A}_{k\sigma, l\mu}^\dagger | \Psi \rangle$, and must therefore be positive. The choice $\hat{A}_{i\sigma, j\mu} = \hat{a}_{i\sigma}^\dagger \hat{a}_{j\mu}$ defines matrix elements of $\hat{D}^{\sigma\mu}$, while $\hat{A}_{i\sigma, j\mu} = \hat{a}_{i\sigma} \hat{a}_{j\mu}$ and $\hat{A}_{i\sigma, j\mu} = \hat{a}_{i\sigma}^\dagger \hat{a}_{j\mu}$, respectively, define matrix elements of $\hat{Q}^{\sigma\mu}$ and $\hat{G}^{\sigma\mu}$. (This is a slightly different *G*-matrix than the one introduced by Garrod and Percus.³⁴) The selection $\hat{A}_{i\sigma, j\mu} = \hat{a}_{i\sigma} \hat{a}_{j\mu}^\dagger$ does not generate an independent positivity condition, as the corresponding metric matrix is positive if and only if $\hat{G}^{\sigma\mu}$ is positive.³⁸

For spin-compensated states, \hat{D} , \hat{Q} , and \hat{G} are completely determined by their $\alpha\alpha$ and $\alpha\beta$ spin blocks. Upon rearranging some creation and annihilation operators, one obtains

$$Q_{ij,kl}^{\alpha\alpha} = D_{kl,ij}^{\alpha\alpha} + \frac{1}{2} [\delta_{lj} (\delta_{ki} - \gamma_{k,i}^\alpha) - \delta_{li} (\delta_{kj} - \gamma_{k,j}^\alpha) + \delta_{kj} \gamma_{l,i}^\alpha - \delta_{ki} \gamma_{l,j}^\alpha], \quad (10)$$

$$Q_{ij,kl}^{\alpha\beta} = D_{kl,ij}^{\alpha\beta} + \frac{1}{2} (\delta_{ik} \delta_{jl} - \gamma_{k,i}^\alpha \delta_{jl} - \gamma_{l,j}^\beta \delta_{ik}), \quad (11)$$

$$G_{ij,kl}^{\alpha\alpha} = -D_{il,kj}^{\alpha\alpha} + \frac{1}{2} \gamma_{i,k}^\alpha \delta_{jl}, \quad (12)$$

and

$$G_{ij,kl}^{\alpha\beta} = -D_{il,kj}^{\alpha\beta} + \frac{1}{2} \gamma_{i,k}^\alpha \delta_{jl}. \quad (13)$$

These expressions are valid in an arbitrary basis of orthonormal orbitals.

Assuming a Hartree-product form for $\hat{D}^{\alpha\beta}$, and introducing the abbreviations

$$H_{ij} = n_i n_j, \quad \Omega_{ij} = 1 - n_i - n_j, \quad (14)$$

one obtains

$$Q_{ij,kl}^{\alpha\beta} = \frac{1}{2} \delta_{ik} \delta_{jl} (H_{ij} + \Omega_{ij}) \quad (15)$$

and

$$G_{ij,kl}^{\alpha\beta} = \frac{1}{2} \delta_{ik} \delta_{jl} \Delta_{ij}. \quad (16)$$

These matrices are diagonal, with eigenvalues $Q_{ij,ij}^{\alpha\beta}$ and $G_{ij,ij}^{\alpha\beta}$ that are non-negative for $0 \leq n_i, n_j \leq 1$. Thus the Hartree-product reconstruction of $\hat{D}^{\alpha\beta}$ satisfies each of the *D*, *Q*, and *G* conditions.

With $\hat{D}^{\alpha\alpha}$ reconstructed according to Eq. (6), one obtains

$$Q_{ij,kl}^{\alpha\alpha} = \frac{1}{2} \delta_{ik} \delta_{jl} (H_{ij} + \Omega_{ij}) - \frac{1}{2} \delta_{il} \delta_{jk} [f(n_i, n_j) + \Omega_{ij}] \quad (17)$$

and

$$G_{ij,kl}^{\alpha\alpha} = \frac{1}{2} \delta_{ik} \delta_{jl} [n_i - f(n_i, n_j)] + \frac{1}{2} H_{ik} \delta_{ij} \delta_{kl}. \quad (18)$$

TABLE II. Eigenvalues of $\hat{D}^{\alpha\alpha}$, $\hat{Q}^{\alpha\alpha}$, and $\hat{G}^{\alpha\alpha}$.

Functional	$d_i = q_i$	d_{ij}^-	$d_{ij}^+ = q_{ij}^+$	q_{ij}^-	g_{ij}
CH(ζ)	$(n_i^2 - n_i^{\zeta})/2$	$(H_{ij} + H_{ij}^{\zeta/2})/2$	$(H_{ij} - H_{ij}^{\zeta/2})/2$	$\Omega_{ij} + (H_{ij} + H_{ij}^{\zeta/2})/2$	$(n_i - H_{ij}^{\zeta/2})/2$
SIC-CH(ζ)	0	$(H_{ij} + H_{ij}^{\zeta/2})/2$	$(H_{ij} - H_{ij}^{\zeta/2})/2$	$\Omega_{ij} + (H_{ij} + H_{ij}^{\zeta/2})/2$	$(n_i - H_{ij}^{\zeta/2})/2$
CHF(ζ)	$-\zeta \Delta_{ij}/2$	$H_{ij} + \zeta \sqrt{\Delta_{ii} \Delta_{jj}}/2$	$-\zeta \sqrt{\Delta_{ii} \Delta_{jj}}/2$	$\Omega_{ij} + H_{ij} + \zeta \sqrt{\Delta_{ii} \Delta_{jj}}/2$	$(\Delta_{ij} - \zeta \sqrt{\Delta_{ii} \Delta_{jj}})/2$
MCHF	$-\Delta_{ij}/2$	$(3H_{ij} + \sqrt{\Lambda_{ii} \Lambda_{jj}})/4$	$(H_{ij} - \sqrt{\Lambda_{ii} \Lambda_{jj}})/4$	$\Omega_{ij} + (3H_{ij} + \sqrt{\Lambda_{ii} \Lambda_{jj}})/4$	$(2n_i - H_{ij} - \sqrt{\Lambda_{ii} \Lambda_{jj}})/4$

These matrices, along with $\hat{D}^{\alpha\alpha}$, exhibit a simple block structure that allows us to obtain most of their eigenvalues analytically.

Consider $\hat{D}^{\alpha\alpha}$ first. Its only nonzero elements have the form $D_{ij,ij}^{\alpha\alpha}$ and $D_{ij,ji}^{\alpha\alpha}$, thus $\hat{D}^{\alpha\alpha}$ consists entirely of 1×1 blocks ($D_{ii,ii}^{\alpha\alpha}$) and 2×2 blocks

$$\mathbf{B}_{ij} = \begin{pmatrix} D_{ij,ij}^{\alpha\alpha} & D_{ij,ji}^{\alpha\alpha} \\ D_{ji,ij}^{\alpha\alpha} & D_{ji,ji}^{\alpha\alpha} \end{pmatrix}. \quad (19)$$

The 1×1 blocks contribute eigenvalues

$$d_i \equiv D_{ii,ii}^{\alpha\alpha} = \frac{1}{2}[n_i^2 - f(n_i, n_i)], \quad (20)$$

while \mathbf{B}_{ij} has eigenvalues

$$d_{ij}^{\pm} = \frac{1}{2}[n_i n_j \mp f(n_i, n_j)]. \quad (21)$$

The complete set of $\hat{D}^{\alpha\alpha}$ eigenvalues is $\{d_i\} \cup \{d_{ij}^{\pm} | i < j\}$. The eigenvalue d_i is associated with the eigenvector $|\varphi_i \varphi_i\rangle$, while d_{ij}^{\pm} is associated with the eigenvector $(|\varphi_i \varphi_j\rangle \pm |\varphi_j \varphi_i\rangle)/\sqrt{2}$.

$\hat{Q}^{\alpha\alpha}$ has the same block structure as $\hat{D}^{\alpha\alpha}$. Eigenvalues arising from the 1×1 blocks are the same as for $\hat{D}^{\alpha\alpha}$, $q_i = d_i$, while the 2×2 blocks yield eigenvalues $q_{ij}^+ = d_{ij}^+$ and

$$q_{ij}^- = \Omega_{ij} + \frac{1}{2}[n_i n_j + f(n_i, n_j)]. \quad (22)$$

Last, $\hat{G}^{\alpha\alpha}$ consists of 1×1 blocks, along with a single $R \times R$ block, where R is the number of orbitals. The latter has elements

$$G_{ii,jj}^{\alpha\alpha} = \frac{1}{2}[n_i n_j + \delta_{ij}[n_i - f(n_i, n_i)]]. \quad (23)$$

The 1×1 blocks have elements $G_{ij,ij}^{\alpha\alpha}$, for $i \neq j$, and thus yield eigenvalues

$$g_{ij} = \frac{1}{2}[n_i - f(n_i, n_j)]. \quad (24)$$

In summary, we have analytic expressions for all eigenvalues of \hat{D} , \hat{Q} , and \hat{G} except those arising from a single $R \times R$ block of $\hat{G}^{\alpha\alpha}$. Functional-specific expressions for d_i , d_{ij}^{\pm} , q_{ij}^- , and g_{ij} are compiled in Table II. It follows that $d_{ij}^{\pm} \geq 0$ for each functional, since f , Δ_{ij} , and Λ_{ij} are each non-negative on the domain of allowed occupation numbers. Because $\Omega_{ij} + H_{ij}/2 \geq 0$, it also follows that $q_{ij}^- \geq 0$ for each functional. Consequently, these functionals satisfy the Q condition if and only if they satisfy the D condition.

Unfortunately, all of the functionals listed in Table I violate the D condition. For any $\zeta > 0$, both CHF(ζ) and MCHF have $d_i \leq 0$ and $d_{ij}^+ \leq 0$ for all values of n_i and n_j . These inequalities are strict except in the case of integer occupancies. For CH(ζ), $d_i \leq 0$ and $d_{ij}^+ \leq 0$ for any $\zeta \leq 2$, again with strict inequalities for fractional occupancies. Finally, SIC-

CH(ζ) has the same eigenvalues as CH(ζ), except that $d_i \equiv 0$ in the former (by construction). Thus for each of these functionals, half of the eigenvalues of $\hat{D}^{\alpha\alpha}$ will always be negative. Though the analytic formulas in Table II can be used to place rigorous bounds on the magnitudes of any negative eigenvalues, for spin-compensated systems these theoretical lower bounds are unlikely to be approached in practice, given that the reconstructed D , Q , and G matrices are each positive in the limit of an idempotent 1-matrix. Negative eigenvalues arising in applications are examined in Sec. V.

IV. VARIATIONAL PROCEDURE

In contrast to HF theory, minimization of a more general density matrix functional with fractional occupation numbers cannot be cast as a self-consistent eigenvalue problem. Instead, direct minimization of $E[\{n_i\}, \{|\varphi_i\rangle\}]$ is required, subject to the constraints $0 \leq n_i \leq 1$, $\sum_i n_i = N/2$, and $\langle \varphi_i | \varphi_j \rangle = \delta_{ij}$. This section describes our algorithm for carrying out this optimization, which differs from previous procedures^{27,40-42} in several important respects. These differences are pointed out in the description that follows.

Bounds on the occupation numbers are enforced by setting $n_i = (\cos \omega_i)^2$ and varying the ω_i without constraint. The trace constraint is implemented by optimizing the penalized energy function

$$\tilde{E} = E + K \left(N - 2 \sum_i n_i \right)^2, \quad (25)$$

in which K is a large, positive constant. Having optimized \tilde{E} for a particular value of K , the energy can be reoptimized rapidly using a larger value of K , in order to improve the trace, since very little rate-limiting orbital reoptimization is required.

An alternative to a penalty function is to parametrize the vector of occupation numbers in a manner that automatically preserves the trace.⁴⁰ In our experience, however, freedom to violate the trace constraint accelerates convergence by enabling relatively large changes in the occupation numbers at early stages in the optimization. Furthermore, relaxation of the trace constraint can be crucial as a means to extricate the optimization from a local minimum that is not the global minimum.

Analytic derivatives

$$\frac{\partial E}{\partial \omega_i} = -(\sin 2\omega_i) \frac{\partial E}{\partial n_i} \quad (26)$$

are easily computed, but we find them unnecessary and not cost effective. Note that $\partial E/\partial \omega_i = 0$ if n_i is an integer. As such, we typically initiate the optimization using HF orbitals but using occupation numbers that are perturbed slightly from their HF values.

Orbital optimization, subject to orthonormality constraints, is carried out in a manner similar to that used to perform diagonalization-free self-consistent-field calculations.^{43–49} The natural orbitals $|\varphi_i\rangle$ are represented in terms of some fixed, orthonormal basis set,

$$|\varphi_i\rangle = \sum_j C_{ij} |\psi_j\rangle, \quad (27)$$

with initial guess coefficients that form an orthogonal matrix \mathbf{C} . Any variation $\tilde{\mathbf{C}} = \mathbf{C} + \delta\mathbf{C}$ that preserves orthonormality can be parametrized as

$$\tilde{\mathbf{C}} = \exp(\mathbf{A})\mathbf{C} \approx (\mathbf{I} + \mathbf{A} + \frac{1}{2}\mathbf{A}^2)\mathbf{C}, \quad (28)$$

where $\mathbf{A} = -\mathbf{A}^\top$ is a skew-symmetric matrix of auxiliary variational parameters. We vary the A_{ij} , for fixed \mathbf{C} and fixed occupation numbers, so as to minimize \tilde{E} , which is evaluated at each optimization step using the orbital coefficients \tilde{C}_{ij} . Only when $i < j$ does A_{ij} constitute an independent variational parameter, which we denote by a_{ij} . Then using the fact that $\partial A_{mn}/\partial a_{kl} = \delta_{mk}\delta_{nl} - \delta_{ml}\delta_{nk}$, one obtains orbital gradients

$$\frac{\partial \tilde{E}}{\partial a_{ij}} = \sum_{mn} \frac{\partial \tilde{E}}{\partial \tilde{C}_{mn}} \left(\frac{\partial \tilde{C}_{mn}}{\partial A_{ij}} - \frac{\partial \tilde{C}_{mn}}{\partial A_{ji}} \right), \quad (29)$$

where $i < j$ is assumed but the summation indices are unrestricted. As indicated in Eq. (28), we truncate $\exp(\mathbf{A})$ at second order, which allows us to evaluate the derivatives $\partial \tilde{C}_{mn}/\partial A_{ij}$ in closed form. This approximation notwithstanding, $\tilde{\mathbf{C}}$ is orthogonal and therefore the derivatives $\partial \tilde{E}/\partial \tilde{C}_{mn}$ can be evaluated directly from the energy functional, whereas the derivatives $\partial \tilde{E}/\partial C_{mn}$ cannot.

Let us digress briefly to compare this method to an alternative technique^{15,27,50} in which the expansion coefficients C_{ij} are varied directly. As a result \mathbf{C} is not orthogonal during the course of the optimization, but for sufficiently small variations an orthogonal matrix $\tilde{\mathbf{C}}$ is obtained by first-order symmetric orthogonalization,

$$\tilde{\mathbf{C}} = \mathbf{C}(\mathbf{C}^\top \mathbf{C})^{-1/2} \approx \frac{3}{2}\mathbf{C} - \frac{1}{2}\mathbf{C}\mathbf{C}^\top \mathbf{C}. \quad (30)$$

This relationship is then used to encode the orthogonality constraints into the gradient, via the chain rule

$$\frac{\partial \tilde{E}}{\partial C_{ij}} = \sum_{mn} \frac{\partial \tilde{E}}{\partial \tilde{C}_{mn}} \frac{\partial \tilde{C}_{mn}}{\partial C_{ij}}. \quad (31)$$

As before, the derivatives $\partial \tilde{E}/\partial \tilde{C}_{mn}$ are obtained directly from the energy functional, while $\partial \tilde{C}_{mn}/\partial C_{ij}$ is gleaned from Eq. (30).

For R orbitals, the symmetric orthogonalization scheme employs R^2 variational parameters for the orbital optimization (which is the rate-limiting step), compared to $R(R$

$-1)/2$ for the exponential parametrization. Both methods preserve orthogonality only in the limit of infinitesimal steps, though we find this restriction to be much less severe in the case of the exponential parametrization, presumably because we use a second-order approximation to $\exp(\mathbf{A})$ as compared to the first-order approximation to $(\mathbf{C}^\top \mathbf{C})^{-1/2}$ in Eq. (30). As corroborated by Cohen and Baerends,²⁷ when the first-order symmetric orthogonalization scheme is used, we find that the orbital coefficient matrix must be reorthogonalized, via iterative application of Eq. (30), each time the C_{ij} are updated. Using the exponential parametrization, 10–30 updates to \mathbf{A} can be made, at early stages in the optimization, before the matrix $\tilde{\mathbf{C}} = (\mathbf{I} + \mathbf{A} + \mathbf{A}^2/2)\mathbf{C}$ deviates from orthogonality by more than 10^{-6} , as judged by the matrix elements of $|\tilde{\mathbf{C}}^\top \tilde{\mathbf{C}} - \mathbf{I}|$. In the vicinity of the minimum, \mathbf{A} can be updated 100–200 times before this threshold is breached. It is only at this point that we reorthogonalize, using a few iterations of Eq. (30). These intermediate orthogonalizations are deleterious to the orbital optimization, as they degrade the quality of the iteratively constructed inverse Hessian and thus adversely affect the selection of a line search direction. It is therefore significant that the second-order exponential parametrization can maintain orthogonality over a large number of optimization steps. This robustness explains why we find this parametrization to be more stable than first-order methods based on either symmetric orthogonalization or the exponential parametrization.

The choice of orthogonalization method is also important. Arguably, the most widely disseminated numerical orthogonalization technique is singular value decomposition,⁵¹ which in most implementations utilizes row and column permutations for greater numerical stability. This kind of pivoting, however, produces an orthogonal matrix that frequently bears little resemblance to the original matrix, even if the latter was nearly orthogonal. This has devastating consequences within an optimization algorithm. In contrast, the first-order scheme in Eq. (30) is more benign and does not alter the coefficient matrix too much, provided that this matrix is almost orthogonal.

For definiteness, we list our complete optimization algorithm for $E[\hat{\gamma}]$.

- (1) Minimize $\tilde{E}(\omega_1, \dots, \omega_R)$ for a fixed set of orbitals, using Powell's quadratically convergent algorithm,⁵¹ typically without analytic first derivatives.
- (2) For fixed occupation numbers (including any residual trace error), optimize the orbitals using the Broyden–Fletcher–Goldfarb–Shanno (BFGS) variable metric algorithm.⁵¹
 - (a) Pass $\mathbf{A} = \mathbf{0}$ and an orthogonal matrix \mathbf{C} to the BFGS subroutine. \mathbf{C} is not changed within this routine.
 - (b) Update the parameters a_{ij} by a single BFGS step, using the derivatives in Eq. (29), and thereby update the matrix $\tilde{\mathbf{C}}$ according to Eq. (28).
 - (c) If the BFGS procedure has converged, or if any element of $|\tilde{\mathbf{C}}^\top \tilde{\mathbf{C}} - \mathbf{I}|$ exceeds a specified tolerance, proceed to step 3. Otherwise repeat step 2b.
- (3) Set $\mathbf{C} = \tilde{\mathbf{C}}$ and $\mathbf{A} = \mathbf{0}$, then return to the main program.

TABLE III. FCI energies for basis sets used in this study.

Basis set	$E/\text{hartree}$	
	Be	LiH
STO-6G	-14.541 904	-7.972 331
6-31G	-14.613 545	
6-31G*	-14.616 635	-8.003 126
6-31+G**		-8.009 185
6-311G	-14.632 864	-8.019 522
6-311G(.3p) ^a		-8.035 533
6-311G(d,2p)		-8.035 875
6-311G+(d,3p)		-8.036 749
6-311G(2d)	-14.633 952	
6-311G(2df)	-14.640 254	

^aContains polarization functions on the H atom only.

Orthogonalize \mathbf{C} by iterative application of Eq. (30), then return to step 2. Repeat this cycle until the orbitals are converged.

- (4) If either the orbital or the occupancy optimization resulted in a significant energy change, then transform the integrals to the current natural orbital basis, set $\mathbf{C}=\mathbf{I}$, and return to step 1.
- (5) Once \tilde{E} is converged with respect to all variational parameters, check the value of the penalty function. If its absolute value is greater than or comparable to the energy convergence criterion, increase the value of K (typically by a factor of 100) and return to step 1.

The sole purpose of the integral transformation in step 4 is to accelerate optimization of the n_i . By virtue of this transformation, \mathbf{C} is always equal to an identity matrix within the occupancy-optimization subroutine. Formally, the integral transformation increases the method's scaling to $O(R^5)$, though at present (with HF orbitals as the initial guess), this transformation is facile relative to the orbital optimization and provides a compelling incentive to decouple the orbital- and occupancy-optimization steps, which more than compensates for the fact that these two optimizations must be iterated when performed separately. In fact, it is sometimes advantageous to abort the orbital optimization (at step 3) prior to convergence, then transform the integrals, reoptimize the occupation numbers, and finally begin the orbital optimization anew. In our implementation, this is done whenever the orbitals have been reorthogonalized 5–10

times (typically corresponding to several hundred BFGS updates) without locating a minimum. There is no mention of an intermediate integral transformation in the existing literature^{4,27,32,40–42} on orbital optimization in DMFT, probably because previous studies have focused on smaller basis sets than the ones employed here.

In the special case of the HF functional, one may set to zero all of the a_{ij} except those that couple occupied and virtual orbitals. This reduces the number of orbital parameters from $R(R-1)/2$ to $N(R-N)$ and makes HF calculations facile relative to DMFT. The optimizations performed here bear more similarity, at the algorithm level, to multiconfigurational self-consistent-field (MCSCF) calculations.⁴⁸

V. NUMERICAL RESULTS AND DISCUSSION

In this section we present calculations for Be and LiH in a variety of basis sets, and compare DMFT to FCI correlation energies ($E_c = E - E_{\text{HF}}$). The FCI calculations were carried out with the GAMESS program,⁵² and we utilize standard Pople-type basis sets⁵³ of contracted Gaussian orbitals, available by keyword in GAMESS. These are listed in Table III along with the FCI energy corresponding to each. For both systems, the largest basis set consists of 35 orbitals. In contrast to several previous studies,^{4,27,42} we do not freeze any orbitals or occupation numbers.

A. Variational stability

Optimized correlation energies for Be, and for LiH at its experimental⁵⁴ bond length, are listed in Table IV, while Figs. 1–4 compare the DMFT energies to the FCI ones. Consistent with other results,⁴² the CHF(0.7) functional converges to the HF solution in each case. (This is not true for LiH at stretched bond lengths, as discussed below.) The CH(4/3) and SIC-CH(4/3) functionals recover very little correlation energy (Figs. 3 and 4), yield near-integer occupancies, and are generally quite similar to HF, except at very large Li–H distance.

Figures 1 and 2 present a bit of good news. There, absolute energies obtained from DMFT are plotted against the corresponding FCI energies, which provide a measure of basis-set completeness. The CH(4/3) and SIC-CH(4/3) data nearly overlap on the scales in these figures, so the latter are omitted. The DMFT energy for both CH(4/3) and SIC-CH(4/3) exhibits a torpid, HF-like decrease relative to the

TABLE IV. Correlation energies in selected basis sets.

Method	Be $E_c/\text{hartree}$					LiH($R=1.5953 \text{ \AA}$) $E_c/\text{hartree}$				
	6-31G	6-31G*	6-311G	6-311G(2d)	6-311G(2df)	6-31G*	6-31+G**	6-311G	6-311G(.3p)	6-311+G(d,3p)
CH(1)	0.103 988	0.131 558	0.137 328	0.165 444	0.183 728	0.061 616	0.070 708	0.085 927	0.107 866	0.114 548
SIC-CH(1)	0.032 810	0.046 609	0.059 237	0.069 721	0.081 952	0.019 090	0.025 401	0.038 625	0.052 288	0.054 237
CH(4/3)	0.005 442	0.006 006	0.006 592	0.006 929	0.007 375	0.001 996	0.002 215	0.003 211	0.004 092	0.004 209
SIC-CH(4/3)	0.002 800	0.003 275	0.003 909	0.004 181	0.004 585	0.001 197	0.001 283	0.002 161	0.002 758	0.002 834
CHF(1)	0.039 193	0.051 409	0.038 192	0.057 593	0.063 643	0.022 741	0.025 049	0.020 113	0.026 407	0.030 360
CHF(1.12)	0.077 148	0.096 050	0.076 215	0.105 416	0.114 623	0.047 076	0.051 187	0.042 781	0.053 970	0.060 957
MCHF	0.083 740	0.104 986	0.102 355	0.127 157	0.139 585	0.047 556	0.053 536	0.060 306	0.075 435	0.081 224
FCI	0.046 781	0.049 690	0.060 990	0.061 999	0.068 301	0.022 460	0.027 849	0.034 880	0.049 735	0.050 702

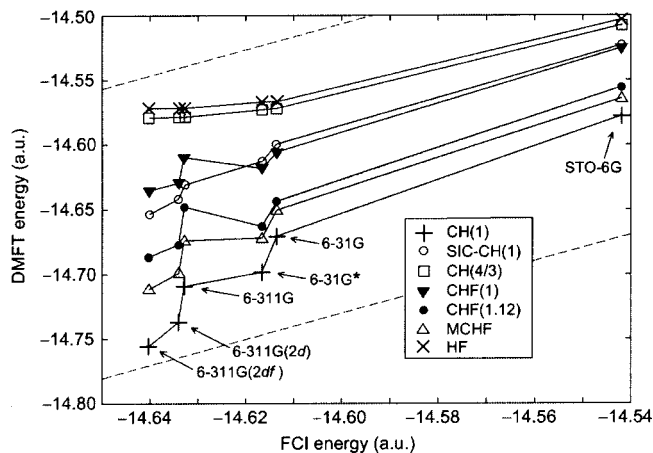


FIG. 1. DMFT vs FCI energies for Be. Dashed guide lines are drawn parallel to the line $E(\text{DMFT}) = E(\text{FCI})$.

FCI energy. Remarkably, for the remaining functionals the DMFT energy decreases at a rate that is not greatly different from that of FCI. There is no reason to expect this *a priori*, and in view of our results concerning N -representability, the mere absence of any precipitous drops in the DMFT energy with respect to increasing completeness is reassuring.

Figure 1 also highlights the fact that certain density matrix functionals are quite sensitive to the presence of polarization functions in the basis set, which has been noted previously.⁴² For both LiH and Be, the FCI energy is (coincidentally) 0.016 a.u. lower in the 6-311G basis than in the 6-31G* basis. In contrast, within DMFT the 6-31G* basis set frequently yields a lower energy, and if not then the difference is small. Figure 3, which depicts the quantity $100 \times (E_{\text{DMFT}} - E_{\text{HF}}) / (E_{\text{FCI}} - E_{\text{HF}})$, emphasizes the same point. At the boundary between the double-zeta and triple-zeta sequences of basis sets, the functionals CH(1), CHF(1), CHF(1.12), and MCHF each exhibit a steep drop in the fraction of the FCI correlation energy that is recovered. SIC-CH(1), in contrast, is far less sensitive to the presence of polarization functions.

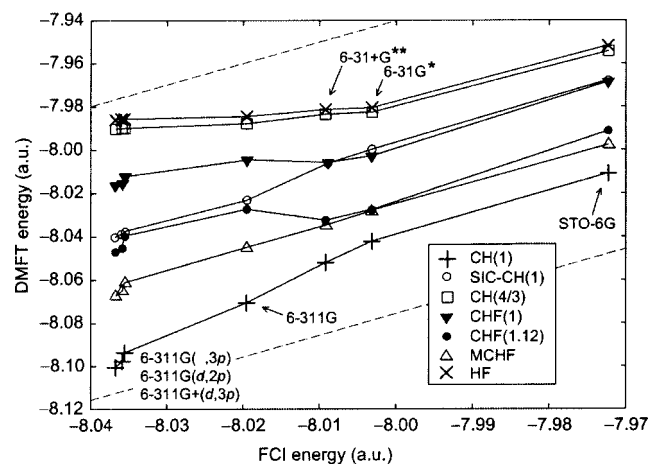


FIG. 2. DMFT vs FCI energies for LiH (at $R = 1.5953 \text{ \AA}$). Dashed guide lines are drawn parallel to the line $E(\text{DMFT}) = E(\text{FCI})$.

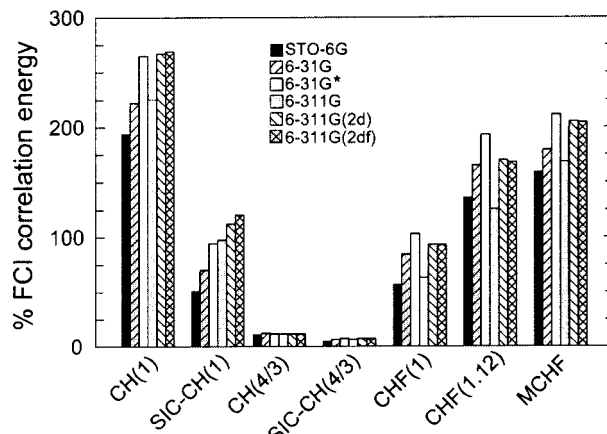


FIG. 3. Be correlation energies, as fractions of the FCI correlation energy.

Optimized occupation numbers for Be are listed in Table V. Atomic Be is an interesting test case on account of a near-degeneracy between the $2s$ and $2p$ manifolds, which leads to an anomalously large FCI occupation number (~ 0.03) in the virtual space. SIC-CH(1), CH(4/3), and SIC-CH(4/3) each reproduce this phenomena at a qualitative level, but the CHF(ζ) and MCHF functionals shift far too much occupancy into the virtual orbitals. In LiH, the CHF(ζ) and MCHF occupation numbers also deviate significantly from integer values, as shown in Fig. 5.

The plots of DMFT versus FCI energy for LiH (Fig. 2) are smoother than the corresponding plots for Be (Fig. 1), and the three LiH data points representing polarized, triple-zeta basis sets are nearly coincident. However, full potential energy curves reveal important differences among basis sets. Figures 6 and 7 compare LiH potential curves obtained with the STO-6G, 6-31G*, and 6-311G(,3p) basis sets. In the minimal basis set, each functional produces a reasonable potential curve, though certain differences are evident at large internuclear distances, as detailed below. For larger basis sets, however, the CH(1), CHF(ζ), and MCHF potentials are far too shallow. [CHF(0.7) and CHF(1.12) results are not shown, but are similar to CHF(1) in this respect.]

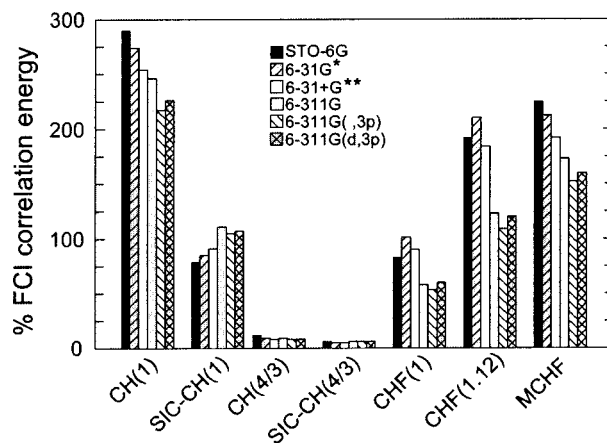


FIG. 4. LiH correlation energies (at $R = 1.5953 \text{ \AA}$), as fractions of the FCI correlation energy.

TABLE V. Largest occupations numbers for Be, up to degeneracy and excluding a unit-occupied core orbital.

Method	STO-6G	6-31G*	6-311G	6-311G (2d)	6-311G (2df)
CH(1)	0.793	0.704	0.728	0.673	0.658
	0.103	0.088	0.080	0.090	0.093
SIC-CH(1)	0.982	0.961	0.963	0.952	0.948
	0.009	0.010	0.009	0.011	0.011
CH(4/3)	0.987	0.984	0.984	0.983	0.983
	0.006	0.005	0.005	0.005	0.005
SIC-CH(4/3)	0.996	0.995	0.994	0.994	0.994
	0.002	0.002	0.002	0.002	0.002
CHF(1)	0.762	0.631	0.667	0.605	0.590
	0.119	0.117	0.107	0.119	0.121
CHF(1.12)	0.672	0.551	0.582	0.526	0.512
	0.164	0.141	0.133	0.140	0.141
MCHF	0.772	0.669	0.697	0.637	0.621
	0.114	0.101	0.092	0.104	0.106
FCI	0.912	0.903	0.905	0.908	0.909
	0.044	0.032	0.031	0.030	0.030

With the beneficial hindsight of these all-electron calculations, the same defect is just barely perceptible in the active-space LiH/CHF(1) potential curves calculated by Cohen and Baerends.²⁷ These authors observe that the CHF(1) potential becomes more shallow as the number of active orbitals is increased from three to five, which they interpret as possible evidence of variational instability. However, we observe no further qualitative change upon incorporating additional polarization or diffuse functions [e.g., enlarging the basis to 6-311+G(*d*,3*p*)], and thus we conclude that the changes observed by Cohen and Baerends are artifacts of a minimal basis (or minimal active space). The shallow potential curves illustrated in Figs. 6 and 7 for extended basis sets are similar to those obtained for other diatomic molecules using the same functionals,^{32,42} and we believe that this is the true nature of diatomic potentials for these functionals.

In contrast to the ill behavior of CH(1), CHF(ζ), and MCHF, the functionals SIC-CH(1), CH(4/3), and SIC-CH(4/3) produce reasonable potential curves in each basis set. The latter two functionals yield near-HF potentials, except at large internuclear separation, while the SIC-CH(1) potentials (Fig. 6) are actually quite close to the FCI ones at moderate Li-H distance. The dissociative asymptote for

SIC-CH(1) is much too high in the minimal basis but is significantly improved in the other basis sets.

LiH/6-311G(\cdot ,3*p*) potential curves for SIC-CH(1), CHF(0.7), and CHF(1) are compared in Fig. 8. The behavior of the CHF functionals here is especially interesting. For $R \lesssim 1.5R_e$, CHF(0.7) converges to the HF energy, but at large bond lengths the CHF(0.7) potential curve is vastly superior to the HF one. Not only is the asymptotic energy lower than HF, but the inflection point in the potential occurs at a shorter bond length, leading to a more realistic shape. CHF(0.7) is also superior to SIC-CH(1) in this respect; although the SIC-CH(1) potential is quite close to FCI for $R \lesssim 2R_e$, SIC-CH(1) turns over too slowly in the asymptotic region. There is nothing special about $\zeta=0.7$ in this regard; $\zeta=0.65$ and $\zeta=0.75$, for example, yield similar diatomic potential curves.³² Although it is probably a coincidence, for a sufficiently large basis CHF(1) produces a potential curve that is almost purely repulsive, but whose asymptote yields an essentially exact^{55,56} dissociation energy.

Confronted with these facts, it is natural to inquire whether there is some hybrid of SIC-CH(1) and CHF(ζ) that looks mostly like the former at modest bond lengths, yet incorporates the early turnover of the latter in the dissocia-

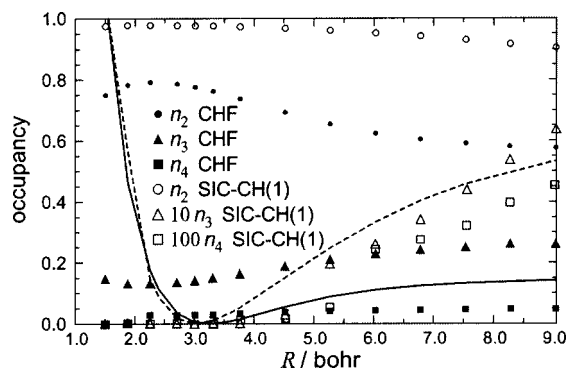


FIG. 5. Largest LiH/6-311G(*d*,2*p*) occupation numbers, up to degeneracy and excluding a unit-occupied core orbital. Also shown are potential curves for the SIC-CH(1) (solid line) and CHF(1) (broken line) functionals, each scaled by the same factor.

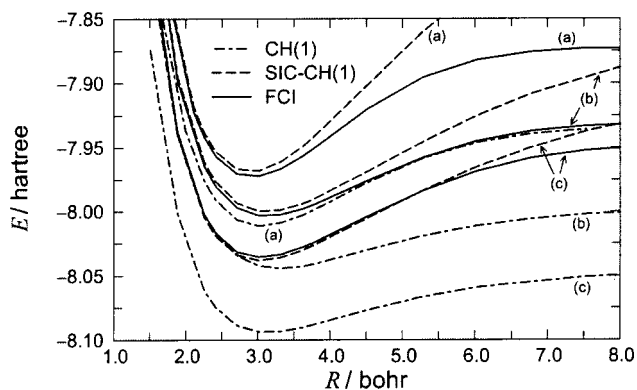


FIG. 6. LiH potential curves obtained with (a) the STO-6G basis, (b) the 6-31G* basis, and (c) the 6-311G(\cdot ,3*p*) basis.

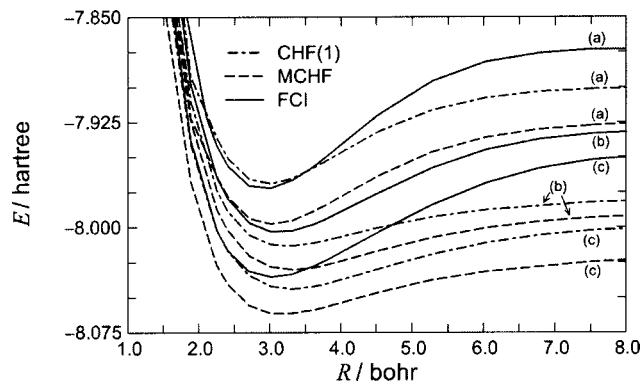


FIG. 7. LiH potential curves obtained with (a) the STO-6G basis, (b) the 6-31G* basis, and (c) the 6-311G(-,3p) basis.

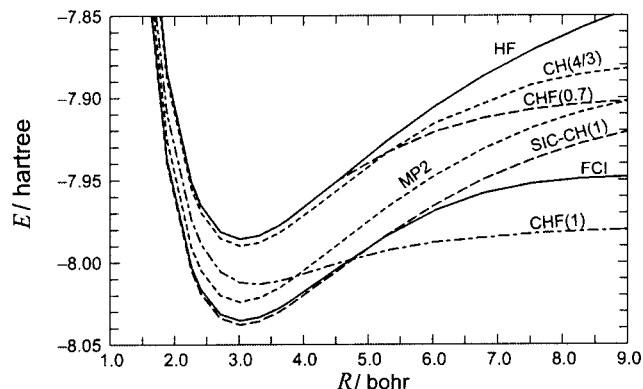


FIG. 8. LiH/6-311G(-,3p) potential curves.

tive regime. No such hybrid has been examined to date, though a hybrid functional

$$E_{\text{hybrid}} = \lambda E_{\text{CH}(1)} + (1 - \lambda) E_{\text{CHF}(1)}, \quad (32)$$

with parameter λ optimized for He atom, has been tested.⁴² We have demonstrated, however, that for a sufficiently large basis neither of these two constituent functionals generates a proper potential energy curve, so it is not surprising that the above hybrid also yields qualitatively incorrect diatomic potentials.

B. N-representability

The spectra of $\hat{D}^{\alpha\alpha}$, $\hat{Q}^{\alpha\alpha}$, and $\hat{G}^{\alpha\alpha}$, reconstructed from variationally optimized 1-matrices, have also been obtained. For all of the functionals except CHF(1.12), we find that the $R \times R$ block ($G_{ii,jj}^{\alpha\alpha}$) of $\hat{G}^{\alpha\alpha}$ is positive. For all remaining eigenvalues we possess analytic formulas (Table II). Of these, d_i and d_{ij}^+ are necessarily negative (or zero) and g_{ij} can also be negative.

Table VI summarizes the spectra of $\hat{D}^{\alpha\alpha}$ and $\hat{G}^{\alpha\alpha}$ obtained for Be in the best basis set utilized here, 6-311G(2df). This basis consists of 35 orbitals, so there are 595 d_{ij}^+ and 1190 g_{ij} eigenvalues. As indicated in the table, most of the d_{ij}^+ are more negative than -10^{-4} , except in the

case of the CH(4/3) and SIC-CH(4/3) functionals. Results for the LiH/6-311G(d,2p) 2-matrix (Table VII) are similar. In this case there are 28 orbitals, hence 378 d_{ij}^+ eigenvalues.

For the functionals considered in this work, we have shown that each 2×2 block \mathbf{B}_{ij} is associated with exactly one negative and one positive eigenvalue. More generally, we suggest that such is likely to be the case in practice (that is, for variationally optimized density matrices) for any ansatz exhibiting this simple block structure, unless negative eigenvalues are somehow excluded by design. To understand why, consider the natural expansion of $\hat{D}^{\alpha\alpha}$, which has the form

$$\begin{aligned} \hat{D}^{\alpha\alpha} = & \sum_i d_i |\varphi_i \varphi_i\rangle \langle \varphi_i \varphi_i| \\ & + \sum_{i < j} \sum_{+,-} d_{ij}^{\pm} (|\varphi_i \varphi_j\rangle \langle \varphi_i \varphi_j| \pm |\varphi_i \varphi_j\rangle \langle \varphi_j \varphi_i|) \end{aligned} \quad (33)$$

for any reconstruction exhibiting the \mathbf{B}_{ij} block structure. $\hat{D}^{\alpha\alpha}$ contributes $2E_2^{\alpha\alpha}$ to the electron repulsion energy, where $E_2^{\sigma\mu} = \text{tr}(r_{12}^{-1} \hat{D}^{\sigma\mu})$, which can be decomposed into a sum of natural geminal pair energies. The pair energies for the natural geminals associated with d_i , d_{ij}^+ , and d_{ij}^- are $\langle ii|ii\rangle$, $\langle ij|ij\rangle + \langle ij|ji\rangle$, and $\langle ij|ij\rangle - \langle ij|ji\rangle$, respectively. Whereas

TABLE VI. Spectrum of $\hat{D}^{\alpha\alpha}$ (first line for each functional) and $\hat{G}^{\alpha\alpha}$ (second line), for Be/6-311G(2df).

Functional	Largest eigenvalue	Most neg. eigenvalue	No. $< -10^{-n}$		
			$n=6$	$n=4$	$n=2$
CH(1)	0.7344	-0.1126	629	602	65
	0.7294	-0.1059	544	433	49
SIC-CH(1)	0.9608	-0.0473	595	438	27
	0.9614	-0.0473	542	291	27
CH(4/3)	0.9860	-0.0121	190	45	6
	0.9848	-0.0121	100	35	6
SIC-CH(4/3)	0.9950	-0.0062	130	33	0
	0.9955	-0.0062	67	33	0
CHF(1)	0.5908	-0.1210	629	492	37
	0.6960	-0.0554	528	312	15
CHF(1.12)	0.5137	-0.1399	630	504	46
	0.6577	-0.0630	672	371	39
MCHF	0.6973	-0.1178	629	602	63
	0.7101	-0.0856	547	390	32

TABLE VII. Spectrum of $\hat{D}^{\alpha\alpha}$ for LiH/6-311G(*d,2p*) at R_e (first line for each functional), $1.5R_e$ (second line), and $3R_e$ (third line).

Functional	Largest eigenvalue	Most neg. eigenvalue	No. $< -10^{-n}$		
			$n=6$	$n=4$	$n=2$
CH(1)	0.8411	-0.1075	405	364	46
	0.7854	-0.1176	405	369	52
	0.6748	-0.1249	405	378	57
SIC-CH(1)	0.9820	-0.0396	378	189	16
	0.9753	-0.0530	378	230	18
	0.9271	-0.0939	378	307	27
CH(4/3)	0.9950	-0.0093	116	27	0
	0.9878	-0.0201	136	33	2
	0.7673	-0.0738	178	51	5
SIC-CH(4/3)	0.9981	-0.0047	83	25	0
	0.9969	-0.0082	90	25	0
	0.9811	-0.0275	134	34	2
CHF(1)	0.7771	-0.0869	406	283	14
	0.6939	-0.1064	406	295	21
	0.5768	-0.1222	406	335	22
CHF(1.12)	0.7048	-0.1169	406	337	25
	0.6348	-0.1301	406	345	29
	0.5489	-0.1388	406	352	43
MCHF	0.8292	-0.0911	405	356	42
	0.7683	-0.1038	405	369	50
	0.6613	-0.1219	405	378	56

$\langle ij|ij\rangle - \langle ij|ji\rangle$ can be positive or negative, the other two pair energies are non-negative; consequently the energy is always lowered by admitting negative eigenvalues for $\hat{D}^{\alpha\alpha}$. Moreover, this unphysical energy lowering occurs by a “direct” mechanism, that is, simply by changing d_i or d_{ij}^+ , without modifying the orbitals.

To quantify the energy lowering attributable to negative eigenvalues of $\hat{D}^{\alpha\alpha}$, we have decomposed each optimized electronic energy into a one-electron part, $2E_1^\alpha = 2\text{tr}(\hat{h}\hat{\gamma}^\alpha)$, and a two-electron part, $2(E_2^{\alpha\alpha} + E_2^{\alpha\beta})$. $E_2^{\alpha\alpha}$ is further decomposed into natural geminal pair energies, as described above. The resulting energy decompositions are

given in Table VIII. Also tabulated is $|\mathfrak{R}|$, where \mathfrak{R} is the ratio of negative- to positive-eigenvalue contributions to $E_2^{\alpha\alpha}$. Except for the near-HF functionals CH(4/3) and SIC-CH(4/3), this ratio ranges from 0.4–0.8, meaning that negative eigenvalues of the 2-matrix annihilate 40%–80% of the parallel-spin electron repulsion energy arising from the positive eigenvalues. In absolute terms, this anomalous energy lowering is huge—frequently a hartree or more. Clearly, the negative eigenvalues of $\hat{D}^{\alpha\alpha}$ are crucial to determining the optimized electronic energy.

As we have indicated, numerous negative 2-matrix eigenvalues are probably to be expected in reconstructive

TABLE VIII. Decomposition of DMFT electronic energies for Be/6-311G(2*df*) (upper data set) and LiH($R=1.5953\text{ \AA}$)/6-311+G(*d,3p*) (lower data set). All values are in hartrees.

Functional	$2E_1^\alpha$	Contributions to $2E_2^{\alpha\alpha}$			$2E_2^{\alpha\beta}$	E	$ \mathfrak{R} $
		From $\{d_i\}$	From $\{d_{ij}^+\}$	From $\{d_{ij}^-\}$			
HF	-19.061 601	0.000 000	0.000 000	0.911 416	3.578 232	-14.571 953	0.00
CH(1)	-18.668 248	-0.157 949	-1.755 649	2.481 845	3.429 023	-14.670 978	0.77
SIC-CH(1)	-18.997 737	0.000 000	-0.784 286	1.606 510	3.559 236	-14.616 277	0.49
CH(4/3)	-19.043 014	-0.004 414	-0.076 264	0.905 666	3.571 371	-14.573 330	0.09
SIC-CH(4/3)	-19.054 487	0.000 000	-0.044 568	0.950 235	3.576 077	-14.572 744	0.05
CHF(1)	-18.611 223	-0.174 828	-0.724 415	1.532 446	3.393 895	-14.584 124	0.59
CHF(1.12)	-18.518 993	-0.216 928	-1.007 801	1.767 850	3.361 121	-14.614 750	0.69
MCHF	-18.633 732	-0.168 191	-1.476 371	2.228 729	3.411 587	-14.637 979	0.74
HF	-12.465 925	0.000 000	0.000 000	0.669 819	2.814 929	-8.981 177	0.00
CH(1)	-12.122 610	-0.118 276	-1.025 775	1.601 107	2.657 043	-9.008 510	0.71
SIC-CH(1)	-12.416 512	0.000 000	-0.509 962	1.114 852	2.811 963	-8.999 659	0.46
CH(4/3)	-12.455 077	-0.002 228	-0.046 952	0.712 088	2.813 598	-8.978 571	0.07
SIC-CH(4/3)	-12.460 630	0.000 000	-0.029 530	0.695 060	2.814 948	-8.980 153	0.04
CHF(1)	-12.069 959	-0.115 591	-0.248 405	0.869 255	2.605 495	-8.959 206	0.42
CHF(1.12)	-11.941 571	-0.159 687	-0.405 064	1.000 109	2.548 057	-8.958 156	0.56
MCHF	-12.308 129	-0.157 320	-1.051 491	1.680 444	2.774 178	-9.062 319	0.72

DMFT, unless specific steps are taken to avoid them. The SIC variant of CH(ζ) takes a step in this direction by removing the $D_{ii,ii}^{\alpha\alpha}$ matrix elements in the natural orbital direct product basis. This annihilates most (though not all) of the self-interaction associated with CH(ζ).⁴ What is more, the remaining negative eigenvalues d_{ij}^+ , which have the same analytic form for both CH(ζ) and SIC-CH(ζ), tend to be closer to zero for the latter functional, and their contribution to the energy is also much reduced in the case of SIC-CH(ζ). Unfortunately, the aforementioned self-interaction correction is basis-set-specific, and consequently the SIC-CH(ζ) energy functional is not invariant to unitary transformations among orbitals with degenerate occupancies.⁴⁰ Thus the energy will generally change if, for example, real linear combinations are substituted for primitive spherical harmonics in any orbitals with nonzero angular momentum.

In contrast to this *ad hoc* procedure for removing self-interaction, any approximate reconstruction functional $\hat{D}^{\alpha\alpha}[\hat{\gamma}]$ that preserves the full antisymmetry of the 2-matrix (not just the symmetry $D_{ij,kl}^{\alpha\alpha} = D_{ji,lk}^{\alpha\alpha}$, which is satisfied by all of the functionals considered here) is completely free of self-interaction, by construction, and does not suffer the aforementioned anomaly in the case of degenerate occupancies. Consider an antisymmetric ansatz for $\hat{D}^{\alpha\alpha}[\hat{\gamma}]$ that consists of the same \mathbf{B}_{ij} block structure as the functionals studied here. There are no 1×1 blocks for such a functional, and each 2×2 block \mathbf{B}_{ij} contains only one independent element and has eigenvalues $2 D_{ij,ij}^{\alpha\alpha}$ and zero. Hence antisymmetry cures the positivity problem, provided that the geminal populations $2 D_{ij,ij}^{\alpha\alpha}$ are themselves positive.

Antisymmetry implies positivity only for extremely sparse 2-matrices with the \mathbf{B}_{ij} block structure. More generally, antisymmetric reconstruction functionals need not eliminate negative eigenvalues of $\hat{D}^{\alpha\alpha}$ altogether, but may avoid large ones, for two reasons. First, elements of the \mathbf{B}_{ij} blocks, which represent geminal populations, should be far larger in magnitude than off-diagonal 2-matrix elements, which represent coherences between geminals. The Schwarz inequality dictates that

$$|D_{ij,kl}^{\alpha\alpha}|^2 \leq D_{ij,ij}^{\alpha\alpha} D_{kl,kl}^{\alpha\alpha}, \quad (34)$$

though in most cases the coherences $D_{ij,kl}^{\alpha\alpha}$ are significantly smaller than this theoretical upper bound. As such, these elements represent small perturbations to the spectrum determined by the \mathbf{B}_{ij} blocks. Second, one finds from Eq. (4) that matrix elements of $\hat{D}^{\alpha\alpha}$ lying outside the \mathbf{B}_{ij} blocks contribute only to off-diagonal elements of the 1-matrix. If $\hat{D}^{\alpha\alpha}$ is reconstructed in the natural orbital product basis, these off-diagonal contributions must sum to zero. Although the off-diagonal elements of $\hat{D}^{\alpha\alpha}$ can be positive or negative, one hopes that this sum rule leads them to be small, in the natural orbital product basis. (The off-diagonal elements of $\hat{D}^{\alpha\alpha}$ will be equal to zero in this basis, if the natural geminals are 2×2 determinants of natural orbitals.)

In view of these remarks, the development of antisymmetric reconstruction functionals should be a priority. Otherwise, it is difficult to see how the negative spectrum of $\hat{D}^{\alpha\alpha}$ can be eliminated or mitigated, within an ansatz bearing any

similarity to the ones examined here. (We mention in this regard that an iterative procedure⁵⁷ for removing negative eigenvalues of \hat{D} , \hat{Q} , and \hat{G} , by adjusting \hat{D} while preserving the underlying 1-matrix, is ineffective in the present case, as there are too few nonzero 2-matrix elements.) In the considerations leading to the CH(1) and CHF(1) functionals,⁵ antisymmetry was abandoned in order to obtain an alternative to the HF functional that still satisfies the contraction relation in Eq. (4), which is thought to be an extremely important N -representability requirement, based on experience with sum rules in DFT. To recover antisymmetry in DMFT, yet still maintain this partial trace relation, it is probably necessary to move beyond one-term tensor product approximations for \hat{D} . For more complicated reconstructions, the contraction relation is not so easy to enforce, though we speculate that perhaps some variant of Perdew's real-space cutoff procedure¹⁸⁻²⁰ might be used in this capacity, much as it is used in DFT to enforce sum rules on the exchange-correlation hole.

VI. CONCLUDING REMARKS

We have documented extensive N -representability violations for proposed reconstructive density matrix functionals. In particular, half of the eigenvalues of $\hat{D}^{\alpha\alpha}$ are necessarily negative for each of the functionals examined in this work. In applications to Be and LiH, we find that the negative eigenvalues significantly lower the electron repulsion energy, often by as much as 1-2 hartrees. While this is certainly an undesirable state of affairs, it is perhaps inappropriate to demand that reconstruction functionals for DMFT exactly comply with all known N -representability requirements for the 2-matrix. Even if this were feasible, it would likely result in a method whose computational cost rivals that of proper variational 2-matrix methods. Instead, we suggest that the more appropriate niche for DMFT is to find models that produce good results (preferably, for identifiable reasons) and are largely free of egregious N -representability violations. To this end, we suggest that explicitly antisymmetric reconstruction functionals should help to correct the positivity problem. Any antisymmetric reconstruction is also rigorously free of self-interaction error. Furthermore, only by employing an antisymmetric ansatz for the 2-matrix can one hope to obtain a correct description of the pair density for parallel-spin electrons, which is poorly described by all of the functionals examined here.²⁸

Despite the pervasive N -representability violations manifested by the current generation of density matrix functionals, we have found no evidence that the electronic energy diverges as the variational space is enlarged, as previous active-space calculations²⁷ have suggested. Rather, this apparent instability appears to be an artifact of a pronounced difference between the shape of diatomic potential curves calculated in a minimal basis set, and those calculated using extended basis sets. Consistent with previous results,^{32,42} our extended-basis calculations demonstrate that the corrected Hartree-Fock-type functionals^{5,6} CHF(ζ) and MCHF are inappropriate for molecular applications. On the other hand, the functional SIC-CH(1) introduced by Goedecker and

Umrigar^{4,15} yields LiH potential curves that are qualitatively correct in all basis sets. As compared to FCI, the SIC-CH(1) potentials are also quite accurate.

Last, let us comment on the practical efficacy of reconstructive DMFT. Computationally speaking, this methodology in its present form is highly evocative of MCSCF theory. Though this analogy will no doubt be useful in developing improved optimization algorithms, in the immediate future it is likely that—like MCSCF methods—this form of DMFT is limited to a few tens of orbitals. Exploratory calculations for Be in a 48-orbital basis required a few days of computer time to optimize fully, starting from HF orbitals. This illustrates the pressing need for starting orbitals that are closer to the optimized ones than are the HF orbitals, which (in the virtual space at least) are exceedingly poor initial guesses and lead to lengthy orbital optimizations. Augmenting the BFGS algorithm with analytic formulas for the diagonal of the Hessian may accelerate the orbital optimization,^{49,58} but even so it seems likely that the future of reconstructive DMFT lies in active-space implementations. Our results indicate, however, that caution must be exercised when appraising density matrix functionals based on active-space results.

ACKNOWLEDGMENTS

One of the authors (J.M.H.) acknowledges the Department of Defense and the IBM corporation for financial support, and thanks Tolga Gulmen for discussions. Computer facilities were provided by the Chemistry Department at the University of Wisconsin, through National Science Foundation Grant No. CHE-0091916 as well as gifts from the Intel corporation.

- ¹For a bibliography of early formal results in DMFT, see M. Levy, in *Density Matrices and Density Functionals*, edited by R. Erdahl and V. H. Smith, Jr. (Reidel, New York, 1987), p. 479.
- ²A. M. K. Müller, Phys. Lett. A **105**, 446 (1984).
- ³A. E. Carlsson, Phys. Rev. B **56**, 12058 (1997).
- ⁴S. Goedecker and C. J. Umrigar, Phys. Rev. Lett. **81**, 866 (1998).
- ⁵G. Csányi and T. A. Arias, Phys. Rev. B **61**, 7348 (2000).
- ⁶G. Csányi, S. Goedecker, and T. A. Arias, Phys. Rev. A **65**, 032510 (2002).
- ⁷M. A. Buijse and E. J. Baerends, Mol. Phys. **100**, 401 (2002).
- ⁸K. Yasuda, Phys. Rev. A **63**, 032517 (2001).
- ⁹K. Yasuda, Phys. Rev. Lett. **88**, 053001 (2002).
- ¹⁰P. J. Hay, J. Chem. Phys. **59**, 2468 (1973).
- ¹¹W. Meyer, J. Chem. Phys. **58**, 1017 (1973).
- ¹²W. Meyer, in *Methods of Electronic Structure Theory*, edited by H. F. Schaefer III (Plenum, New York, 1977), Vol. 3 of *Modern Theoretical Chemistry*, p. 413.
- ¹³A. Holas, Phys. Rev. A **59**, 3454 (1999).
- ¹⁴J. Cioslowski and K. Pernal, J. Chem. Phys. **111**, 3396 (1999).
- ¹⁵S. Goedecker and C. J. Umrigar, in *Many Electron Densities and Reduced Density Matrices*, edited by J. Cioslowski (Plenum, New York, 2000), p. 165.
- ¹⁶D. A. Mazziotti, Phys. Rev. A **65**, 062511 (2002).
- ¹⁷A. J. Coleman, Rev. Mod. Phys. **35**, 668 (1963).

- ¹⁸J. P. Perdew, Phys. Rev. Lett. **55**, 1665 (1985); **55**, 2370(E) (1985).
- ¹⁹J. P. Perdew and Y. Wang, Phys. Rev. B **33**, 8800 (1986); **40**, 3399(E) (1989).
- ²⁰K. Burke, J. P. Perdew, and M. Ernzerhof, Int. J. Quantum Chem. **61**, 287 (1997).
- ²¹M. Ernzerhof, K. Burke, and J. P. Perdew, in *Recent Developments and Applications of Modern Density Functional Theory*, edited by J. M. Seminario (Elsevier, New York, 1996), p. 207.
- ²²K. Burke, J. P. Perdew, and Y. Wang, in *Electronic Density Functional Theory: Recent Progress and New Directions*, edited by J. F. Dobson, G. Vignale, and M. P. Das (Plenum, New York, 1998), p. 81.
- ²³W. Koch and M. C. Holthausen, *A Chemist's Guide to Density Functional Theory*, 2nd ed. (Wiley-VCH, New York, 2001).
- ²⁴A. C. Scheiner, J. Baker, and J. W. Andzelm, J. Comput. Chem. **18**, 775 (1997).
- ²⁵K. S. Raymond and R. A. Wheeler, J. Comput. Chem. **20**, 207 (1999).
- ²⁶J. M. L. Martin, in *Density Functional Theory: A Bridge Between Chemistry and Physics*, edited by P. Geerlings, F. de Proft, and W. Langenaeker (VUB University Press, Brussels, 1999), p. 111.
- ²⁷A. J. Cohen and E. J. Baerends, Chem. Phys. Lett. **364**, 409 (2002).
- ²⁸J. M. Herbert and J. E. Harriman, Int. J. Quantum Chem. **90**, 355 (2002).
- ²⁹R. McWeeny and Y. Mizuno, Proc. R. Soc. London, Ser. A **259**, 554 (1961).
- ³⁰J. M. Herbert and J. E. Harriman, Phys. Rev. A **65**, 022511 (2002).
- ³¹W. Kutzelnigg and D. Mukherjee, J. Chem. Phys. **110**, 2800 (1999).
- ³²V. N. Staroverov and G. E. Scuseria, J. Chem. Phys. **117**, 11107 (2002).
- ³³J. Cioslowski and K. Pernal, Phys. Rev. A **61**, 034503 (2000).
- ³⁴C. Garrod and J. Percus, J. Math. Phys. **5**, 1756 (1964).
- ³⁵C. Garrod, M. V. Mihailović, and M. Rosina, J. Math. Phys. **16**, 868 (1975).
- ³⁶C. Garrod and M. A. Fusco, Int. J. Quantum Chem. **10**, 495 (1976).
- ³⁷M. Nakata, H. Nakatsuji, M. Ehara, M. Fukuda, K. Nakata, and K. Fujisawa, J. Chem. Phys. **114**, 8282 (2001).
- ³⁸D. A. Mazziotti and R. M. Erdahl, Phys. Rev. A **63**, 042113 (2001).
- ³⁹M. Nakata, M. Ehara, and H. Nakatsuji, J. Chem. Phys. **116**, 5432 (2002).
- ⁴⁰J. Cioslowski and K. Pernal, J. Chem. Phys. **115**, 5784 (2001).
- ⁴¹J. Cioslowski and K. Pernal, J. Chem. Phys. **117**, 67 (2002).
- ⁴²V. N. Staroverov and G. E. Scuseria, J. Chem. Phys. **117**, 2489 (2002).
- ⁴³J. Douady, Y. Ellinger, R. Subra, and B. Levy, J. Chem. Phys. **72**, 1452 (1980).
- ⁴⁴J. F. Rico, J. M. Garcia de la Vega, J. I. F. Alonso, and P. Fantucci, J. Comput. Chem. **4**, 33 (1983).
- ⁴⁵T. H. Fischer and J. Almlöf, J. Phys. Chem. **96**, 9768 (1992).
- ⁴⁶J. Hutter, M. Parrinello, and S. Vogel, J. Chem. Phys. **101**, 3862 (1994).
- ⁴⁷A. T. Wong and R. J. Harrison, J. Comput. Chem. **16**, 1291 (1995).
- ⁴⁸G. Chaban, M. W. Schmidt, and M. S. Gordon, Theor. Chem. Acc. **97**, 88 (1997).
- ⁴⁹T. van Voorhis and M. Head-Gordon, Mol. Phys. **100**, 1713 (2002).
- ⁵⁰S. Goedecker and C. J. Umrigar, Phys. Rev. A **55**, 1765 (1997).
- ⁵¹W. H. Press, S. A. Teukolsky, W. T. Vetterling, and B. P. Flannery, *Numerical Recipes in Fortran 77*, 2nd ed. (Cambridge University Press, New York, 1992).
- ⁵²M. W. Schmidt, K. K. Baldrige, J. A. Boatz *et al.*, J. Comput. Chem. **14**, 1347 (1993).
- ⁵³M. J. Frisch, J. A. Pople, and J. S. Binkley, J. Chem. Phys. **80**, 3265 (1984).
- ⁵⁴G. Herzberg, *Molecular Spectra and Molecular Structure I. Spectra of Diatomic Molecules* (Van Nostrand, New York, 1950).
- ⁵⁵M. Tong, P. Jönsson, and C. F. Fischer, Phys. Scr. **48**, 446 (1993).
- ⁵⁶Z.-C. Yan and G. W. F. Drake, Phys. Rev. A **52**, 3711 (1995).
- ⁵⁷D. A. Mazziotti, Phys. Rev. E **65**, 026704 (2002).
- ⁵⁸T. van Voorhis and M. Head-Gordon, J. Chem. Phys. **117**, 9190 (2002).